

**DISLOCATION BIAS REVISITED**, S.I. Golubov (Oak Ridge National Laboratory, *University of Tennessee*), A.V. Barashev (The University of Liverpool, UK), B.N. Singh (*Risø National Laboratory, Denmark*) and R.E. Stoller (Oak Ridge National Laboratory)

## OBJECTIVE

The objective of this work is to investigate the underlying mechanisms that control damage accumulation in irradiated materials. The current focus is on the impact of anisotropic diffusion on the fate of self-interstitial atoms (SIA) and SIA clusters as they diffuse and react under the influence of internal stress fields associated with extended defects such as dislocations and grain boundaries.

## SUMMARY

A diffusion-based model has been developed to predict how anisotropic diffusion influences the SIA-dislocation bias, and comparisons have been made between the behavior of defects that exhibit 1-D and 3-D diffusion. The dislocation capture radius for SIAs undergoing a mixture of 1-D and 3-D diffusion corresponds to higher interaction energy than the thermal energy, as in the case of pure 3-D diffusion. This leads to reduced dislocation bias factors and suggests that it may be possible to categorize the damage accumulation tendency of metals according to relative stability of the SIA crowdion and dumbbell configurations.

## PROGRESS AND STATUS

### I. Introduction

Greenwood, Foreman and Rimmer [1] suggested in 1959 that a preferential absorption of SIAs by dislocations could cause radiation-induced dimensional changes in reactor materials. The phenomenon of void swelling was then discovered by Cawthorne and Fulton [2] in 1967, and the preferential absorption was incorporated into the theoretical model for void swelling, sometimes called the Standard Rate Theory (see [3] for a review), via an empirical parameter,  $B_D$ , that came to be known as the 'dislocation bias factor'. To reproduce experimentally observed swelling rates, the bias factor, the relative excess of SIAs over vacancies absorbed by dislocations, is required to be an order of the order of several percent [4].

The first attempt to determine  $B_D$  by using the elasticity theory for the point defect - dislocation interaction, by solving the diffusion equation with a drift term have been made by Foreman [5], who concluded that the bias was significantly larger than the empirical estimate. Later, Heald [6] obtained an analytical expression for the bias (see next Section) using the solution of Ham [7] in the form presented by Margvelashvili and Saralidze [8].

The estimates [6,9-12] produced using this approach confirmed much higher  $B_D$  values, e.g. ~15% for the bcc iron and ~30% for the fcc copper. Note that, with these bias factors, the maximum swelling rates corresponding to equal sink strengths of voids and dislocations (see next Section), which are equal to  $B_D / 4 \approx 4$  and 8 %/dpa (displacements per atom, (dpa)), have never been observed.

It should be emphasised that, in the approaches described above, no distinction was made between different types of irradiation: ~1 MeV electrons, fission neutrons and heavy ions. It was believed

that the initial damage is produced in the form of Frenkel pairs. Now we understand much better the mechanisms operating under different conditions and make clear distinction between electron and neutron / heavy ion irradiations (see, e.g. [13-15] and references therein for some recent advances in the development of the Production Bias Model (PBM)). In the latter case, the displacement cascades produce one-dimensionally (1-D) migrating SIA clusters, which change qualitatively the reaction kinetics between defects. Most estimates of the bias factor used data obtained in reactor irradiations, but the treatment of the data on swelling in electron-irradiated metals also resulted in  $B_D \approx 2$  to 4% for fcc copper [13,16,17] (data reported by Glowinski [18] were used in [17]), ~2% for pure Fe-Cr-Ni alloys [19], and an orders of magnitude lower values for bcc metals (see, e.g. swelling data in molybdenum [20]).

A few attempts were made to resolve the contradiction described above since early seventies. It was suggested in [21] that the density of jogs, which are traps for point defects, along dislocation lines is very low, and this could lead to decreasing dislocation sink strength. This might work for vacancies, since they have relatively small binding (formation) energy, ~1.2 eV in copper (e.g. [22]), with the dislocation line and can dissociate from dislocation without being absorbed. The SIAs, however, have high formation energy, ~3.6 eV in copper, and could not escape for any reasonable density of jogs at temperatures of practical importance. As a result, the net flux of SIAs to dislocations, hence the value of the bias factor, could only increase with decreasing jog density and could not explain observations.

Recently, Wolfer [12] suggested that the high values of the dislocation bias factor predicted using the elasticity theory in [6,9-11] are correct, whereas the low swelling rates under neutron irradiations were due to intra-cascade recombination of defects. Thus, he ignored experimental and theoretical knowledge on the principal differences of damage mechanisms operating under neutron and electron irradiations. However, even if the dislocation bias were the main driving force for the microstructure evolution under neutron irradiation, his explanation would contradict the low swelling rates found in electron-irradiated samples, where the intra-cascade recombination is absent (see e.g. [14]).

Another attempts are based on the results of MD simulations using empirical potentials, which demonstrated that, even when the SIA dumbbell configuration is the most stable and the SIAs migrate 3-D in the matrix, in the vicinity of an edge dislocation, the crowdion configuration with the axis along the dislocation Burgers vector become most stable and the SIAs have preference to move 1-D [23-26]. The authors of [25] speculated that this might decrease the dislocation capture efficiency for the SIAs since the SIA migration parallel to the dislocation Burgers vector blocks SIA in its vicinity. They did not provide, however, any mechanism supporting their conjecture.

In this paper, we analyze the applicability of the classical approach of calculating the dislocation bias factor by defining the SIA capture volume as that where the SIA interaction energy with dislocation is higher than thermal energy,  $k_B T$  ( $k_B$  is the Boltzmann constant and  $T$  is the absolute temperature). We argue that it is incorrect when the SIA migration is not pure 3-D with the preference to configurations with the axis parallel to the dislocation Burgers vector and to thermally-activated jumps leading to or preserving such configurations. The critical point is that the SIAs moving this way may escape from the 'capture volume', thus reducing the capture efficiency, hence the bias factor.

## RESULTS

### II. Problem characterisation

In this section we describe the mathematical formulation of the problem as it is in the SRT as formulated in [6-12], which we can use for comparison with the following generalised approach.

The stationary diffusion equation for a vacancy ( $\alpha = v$ ) or SIA ( $\alpha = i$ ) is given by

$$\nabla J_\alpha = 0, \quad (1)$$

where the defect flux near an edge dislocation is

$$J_\alpha = -D_\alpha \nabla C_\alpha - \beta D_\alpha C_\alpha \nabla E_\alpha. \quad (2)$$

Here,  $C_\alpha(r)$  is the defect concentration,  $D_\alpha$  is the diffusion coefficient of the mobile defect,  $\beta = (k_B T)^{-1}$ ,  $k_B$  is the Boltzmann constant,  $T$  is the absolute temperature, and  $E_\alpha$  is the interaction energy between the point defect and dislocation. The largest contribution to the long-range interaction arises from the Cottrell size effect [27,28], which, when expressed in polar coordinates  $(r, \varphi)$ , is given by

$$\beta E_\alpha = -L_\alpha \frac{\sin(\varphi)}{r}. \quad (3)$$

Here, the characteristic ranges of the interaction potential,  $L_\alpha$ , are given by

$$L_\alpha = \frac{\mu b(1+\nu)\Delta\Omega_\alpha}{3\pi(1-\nu)k_B T}, \quad (4)$$

where  $\Delta\Omega_\alpha$  is the relaxation volume of the point defect,  $\mu$  and  $\nu$  are the shear modulus and Poisson ratio, respectively. The boundary conditions correspond to a steady state, where the concentrations of point defects near the dislocation core,  $r = r_0$ , and in the midway between dislocations,  $r = R \equiv (\rho_D / \pi)^{1/2}$ , are kept to be constants, corresponding to the thermal-equilibrium (superscript 'th') and volume overage values (superscript '0'):

$$C_\alpha(r_0) = C_\alpha^{\text{th}}, \quad (5)$$

$$C_\alpha(R) = C_\alpha^0. \quad (6)$$

The solution of Eqs. (1)-(6) gives the following expression for the capture efficiency,  $Z_\alpha$ , and the bias factor,  $B_D$

$$Z_\alpha = \frac{2\pi}{\ln(2R/L_\alpha)}, \quad (\alpha = v, i), \quad (7)$$

$$B_D = \frac{Z_i - Z_v}{Z_v} = \frac{\ln(L_i / L_v)}{\ln(2R / L_v)}. \quad (8)$$

The values of  $B_D$  calculated by using this equation for different metals are given in Table 1 in [12]. Note that  $L_\alpha$  can be interpreted as the absorption radii for point defects, since the interaction energy at smaller distances is higher than the thermal energy:  $|E_\alpha(r < L_\alpha)| > k_B T$ . In addition, both  $Z_v$  and  $Z_i$  are of the order of unity, hence one can use  $Z_v = Z_i \approx 1$  everywhere except for the bias.

At relatively high temperature, when the recombination reactions between point defects make negligible contribution to the total defect loss in the system, and if dislocations and voids are the only sinks, the swelling rate driven by the dislocation bias,  $dS / d\phi$  ( $\phi = Gt$  is the irradiation dose in dpa,  $G$  is the damage rate) is given by

$$\frac{dS}{d\phi} \approx B_D \frac{k_C^2 k_{D,v}^2}{(k_C^2 + k_{D,i}^2)(k_C^2 + k_{D,v}^2)}, \quad (9)$$

where

$$k_{D,\alpha}^2 = Z_\alpha \rho_D, \quad (\alpha = i, v) \quad (10)$$

$$k_C^2 = 4\pi \langle R \rangle N, \quad (11)$$

are the sink strengths of dislocations ( $\rho_D$  is the edge dislocation density) and voids (cavities) for 3-D mobile point defects ( $\langle R \rangle$  being the mean void radius and  $N$  the void number density). As can be seen from this equation, the swelling rate depends on the bias factor and some combination of sink strengths of voids and dislocations. The latter assumes its maximum value of 1/4 when  $k_C^2 = k_D^2$  and decreases by 2.5 times when the sink strengths of voids and dislocations differ from each other by an order of magnitude. The observations show that the sink strengths are often close to each other. Hence, to explain the observed smaller swelling rates than predicted by Eqs. (8)-(11), the dislocation sink strength has to be smaller by about two orders of magnitude as compared to that given by Eq. (10). Such a decrease cannot be justified by the features of SIA diffusion near dislocation observed in MD studies in [23-26]. The only obvious way is to make values of  $Z_v$  and  $Z_i$  closer to each other. Taking into consideration the MD results obtained in [23-26], one can expect that the decrease of  $Z_i$  (rather than increase of  $Z_v$ ) should provide the required decrease of the dislocation bias. It is argued below that the 1-D mode of the SIA diffusion does produce such effect.

### III. Analysis

The theory described above assumes 3-D mobile SIAs and vacancies. Our current understanding of the relative stability and the migration modes in metals and alloys has changed significantly since it was formulated in seventies. In the following we describe relevant information and analyse the consequences on the bias factor.

#### A. Properties of SIAs

Quantum mechanical calculations and MD simulations using empirical potentials show that in all nonmagnetic bcc metals the most stable SIA defect configuration has the  $\langle 111 \rangle$  symmetry [29] and migrates 1-D along its axis. In metals in group 5B of the periodic table (V, Nb, Ta), the difference in formation energies of the  $\langle 111 \rangle$  and  $\langle 110 \rangle$  SIA configurations is significant,  $\sim 0.3$ - $0.55$  eV, while for the group 6B metals (Cr, Mo, W) it is smaller,  $\sim 0.01$ - $0.3$  eV. This in turn is fundamentally different from the ferromagnetic bcc  $\alpha$ -Fe, where the  $\langle 110 \rangle$  dumbbell configuration is by far ( $\sim 0.7$  eV [30,31]) the most stable than the  $\langle 111 \rangle$  crowdion. This trend correlates with the observed thermally activated mobility of SIA defects, deduced from the temperatures of the recovery stage 1.

Table 1. Material and point defect parameters: the lattice parameter,  $a_0$ ; shear modulus,  $\mu$ , and the Poisson's ratio,  $\nu$ , from [33]; and melting temperature,  $T_m$ .

| Element | $a_0$ , nm | $\mu$ , GPa | $\nu$ | $\Delta\Omega_v$ | $\Delta\Omega_i$ | $T_m$ , K |
|---------|------------|-------------|-------|------------------|------------------|-----------|
| bcc Mo  | 0.315      | 123         | 0.305 | -0.45            | 0.85             | 2890      |
| fcc Cu  | 0.361      | 55          | 0.324 | -0.25            | 1.45             | 1357      |

In contrast, in the fcc metals, the dumbbell configuration is energetically favourable and the SIAs migrate 3-D in the matrix (e.g. [22]). It has been found, however, that the crowdion configuration with the axis along the dislocation Burgers vector become stable and the SIAs move 1-D in the vicinity of an edge dislocation [23-26]. Hence, the 1-D mobility governs the behaviour of SIAs near dislocations in fcc metals as well. In the next section we consider in more details the bcc molybdenum (Mo) and fcc copper (Cu). We suppose that the stabilisation effect of edge dislocation on the crowdion configuration has the same origin as that for stronger interaction of dislocations with SIA clusters with the Burgers vector parallel to the dislocation Burgers vector. To keep the analysis simple, we use the isotropic elasticity theory [32] for the stress field of an edge dislocation (see Appendix A) and treat SIAs as infinitesimal dislocation loops containing one SIA. The parameters used in calculations are collected in Table 1.

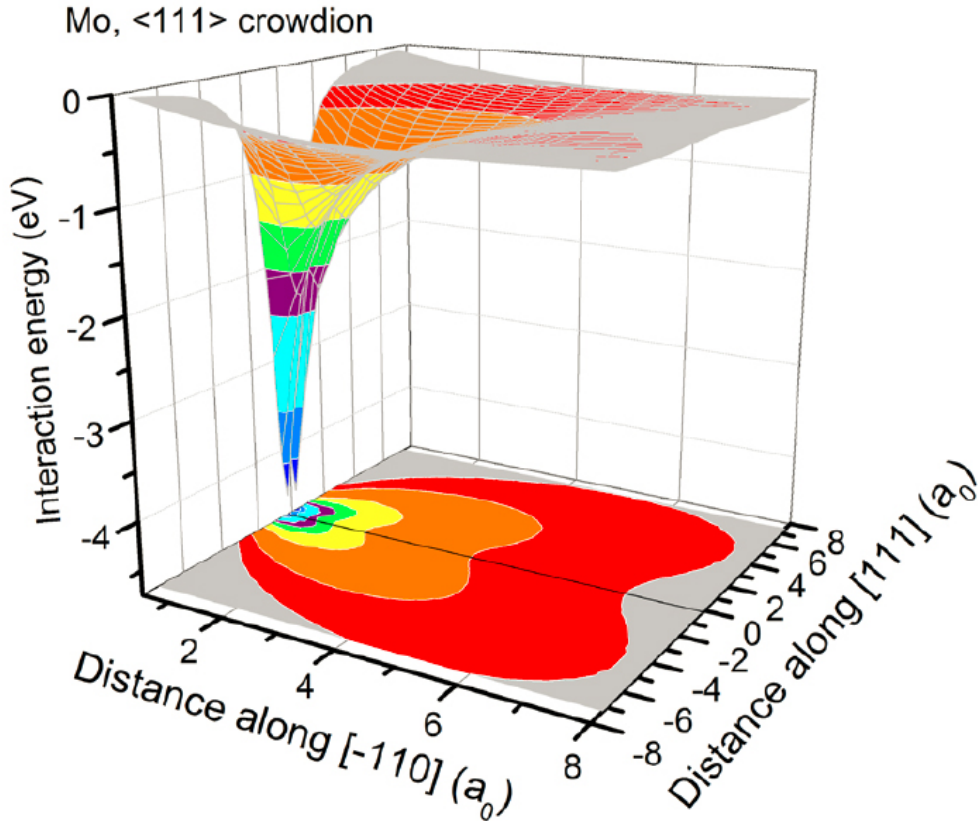


Figure 1. The interaction energy landscape of a  $\frac{1}{2}[111]$  crowdion in the expansion region below the line of a perfect  $\frac{1}{2}[111](\bar{1}10)$  edge dislocation in molybdenum.

## B. Molybdenum

In Mo, the  $\frac{1}{2}\langle 111 \rangle$  crowdion configuration of the SIA is more stable than the dumbbell configuration by  $\sim 0.16$  eV [29]. In the vicinity of the dislocation it is even more stable. This can be seen in Figs. 1 and 2, where the interaction energy landscapes of the crowdion and the SIA in the most stable  $\langle \bar{1}10 \rangle$  dumbbell configuration in the expansion region, below the dislocation line, of a perfect  $\frac{1}{2}[111](\bar{1}10)$  edge dislocation are presented. The interaction energies difference between the crowdion and dumbbell configurations is presented in Fig. 3. As can be seen, it is large except for a narrow area just below the dislocation line, which may be considered as a favourable pass to the dislocation core for migrating dumbbells. However, the realisation of this trajectory is difficult because the dumbbell migrates with changing orientation of its axis, thus deviating from this trajectory. In addition, the configurations with different axes have higher energy (less stable). The energy profiles for the SIAs of different orientations along this pass are presented in Fig. 4. As can be seen, the maximum interaction energy is higher than the thermal energy at a half the melting temperature,  $\frac{1}{2}k_B T_m = 0.125$  eV, in the  $[\bar{1}10]$  direction at a distance of  $\sim 16a_0$  for both  $\langle 111 \rangle$  crowdion and  $\langle \bar{1}10 \rangle$  dumbbell. The interaction energy of dislocation with dumbbells of other orientations is smaller than that of the most stable  $\langle \bar{1}10 \rangle$  configuration, and the difference in the interaction energy increases with decreasing the distance to dislocation. To move towards the dislocation line, the SIA must change from crowdion to dumbbell configuration. If the SIA path towards the dislocation line requires assuming all possible SIA configurations, the activation energy required for such a motion can be estimated as  $\sim 0.2$  eV plus the activation energy of the SIA jump.

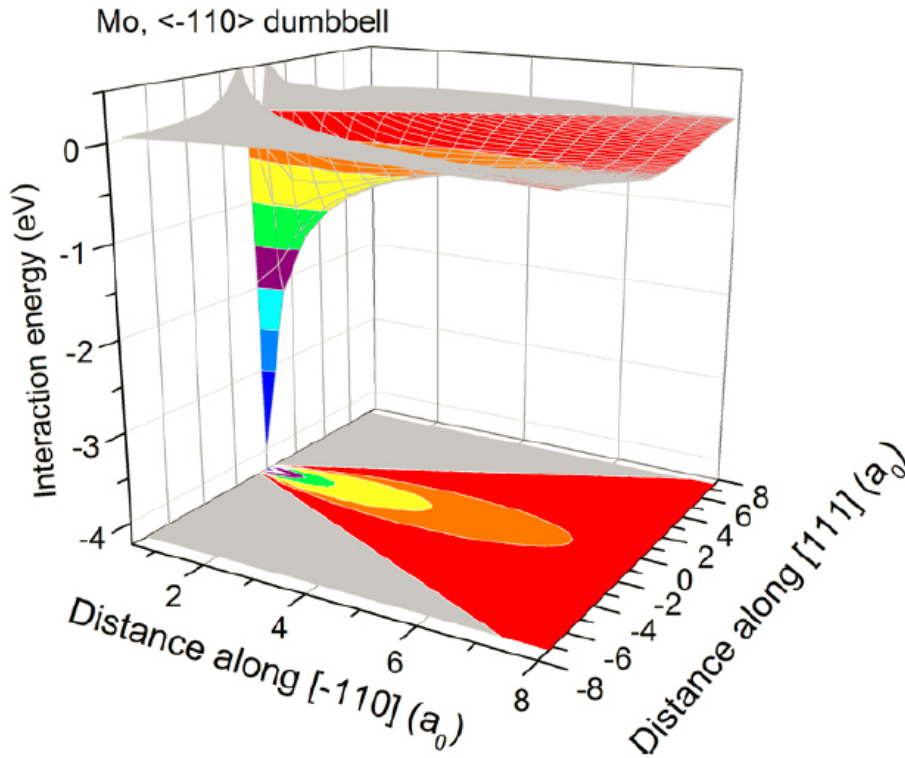


Figure 2. The interaction energy landscape of a  $[-110]$  dumbbell in the expansion region below the line of a perfect  $\frac{1}{2}[111](\bar{1}10)$  edge dislocation in molybdenum.

The energy landscape for a vacancy calculated using Eq. (3) is shown in Fig. 5. It shows that the interaction energy equal to  $\frac{1}{2}k_B T_m$  is achieved at a distance of  $\sim 7.5 a_0$  in the  $[\bar{1}10]$  direction. For 3-D migrating vacancies, the contour corresponding to this energy level can be interpreted as that separating area of free migration of vacancies from that of certain absorption by the dislocation. The same is not correct for the SIAs which have preference to configurations with the axis direction along the dislocation Burgers vector.

The difference in formation energies of the crowdion and dumbbell SIAs far away from dislocation is not so significant and, depending on the temperature, the SIAs can move 3-D with 1-D parts executed while in the crowdion configuration. Near the dislocation, the crowdion configuration parallel to the dislocation Burgers vector is stabilised, which makes it difficult for the SIA to join the dislocation line (see Fig. 4). To estimate the time required for an SIA to be incorporated into dislocation, one needs to know precise details of the SIA migration, which can be obtained by comprehensive studies using combination of first principle, MD and kinetic Monte Carlo (kMC) methods. Below we make some estimates to illustrate the effect.

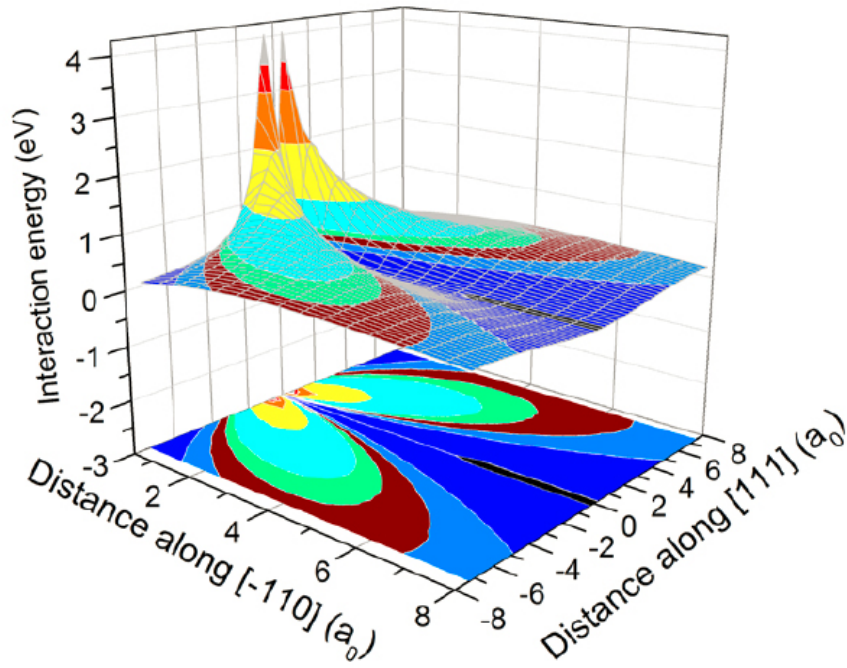


Figure 3. Excess of the interaction energy landscape of a  $\frac{1}{2}[111]$  crowdion compare to that of a  $[-110]$  dumbbell in the expansion region below the line of a perfect  $\frac{1}{2}[111](\bar{1}10)$  edge dislocation in molybdenum.

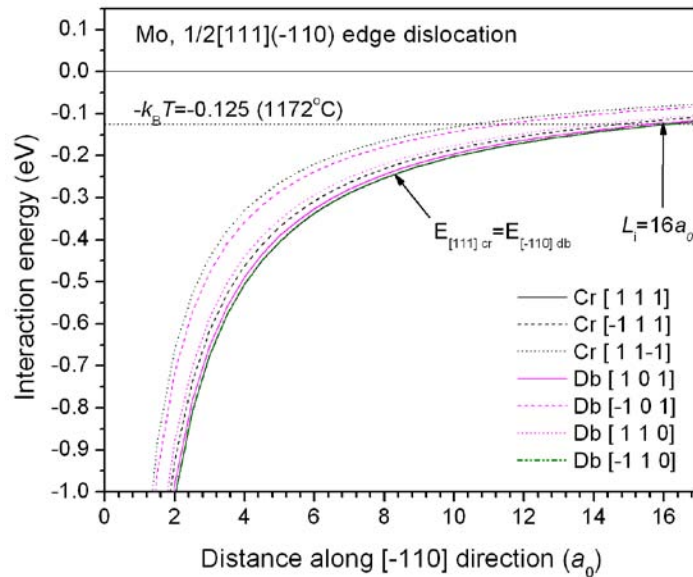


Figure 4. The interaction energy of SIAs of different configurations near  $\frac{1}{2}[111](\bar{1}10)$  edge dislocation in Mo as a function of the distance along  $[\bar{1}10]$  direction.

The SIAs with the Burgers vector parallel to the dislocation Burgers vector can migrate 1-D without being absorbed by the dislocation for a long time. Simple estimates show that this time is not long enough to recombine with incoming vacancies. The mean time,  $t_v$ , between vacancy arrival to a particular point of the dislocation line can be determined from  $Gt_v \approx n\rho_D\Omega$ , where  $\Omega$  is the atomic volume and  $n$  is the linear density of jogs. For  $G=10^{-3}$  dpa/s,  $\Omega=10^{-29}$  m<sup>3</sup>,  $\rho_D=10^{13}$  m<sup>-2</sup> and  $n=0.01/a_0$ ,  $t_v=3\times 10^{-6}$  s. This is much longer than the mean time of the SIA conversion from the crowdion to the dumbbell configuration and migrating towards and absorption by the dislocation line, estimated as



$$t_{\text{ab}} \approx \nu_0^{-1} \exp \left[ \beta \left( E_{\text{db}}^{\text{f}} - E_{\text{cr}}^{\text{f}} + E_{\text{db}}^{\text{m}} \right) \right], \quad (12)$$

where  $\nu_0$  is the attempt frequency  $\sim 10^{12} \text{ s}^{-1}$ ,  $E_{\text{db}}^{\text{f}}$  and  $E_{\text{cr}}^{\text{f}}$  are the dumbbell and crowdion formation energies, respectively, and  $E_{\text{db}}^{\text{m}}$  is the dumbbell migration energy (all energies should be influenced by the proximity to the dislocation). For  $k_{\text{B}}T = 0.05 \text{ eV}$  and  $E_{\text{db}}^{\text{f}} - E_{\text{cr}}^{\text{f}} + E_{\text{db}}^{\text{m}} = 0.3 \text{ eV}$ ,  $t_{\text{ab}} \sim 10^{-10} \text{ s}$ . This time can also be significantly longer than the time required for the SIA in the crowdion configuration to leave the dislocation region, which can be found from

$$t_{\text{leave}} \approx \nu_0^{-1} \exp \left( \beta E_{\text{cr}}^{\text{b}} \right), \quad (13)$$

where  $E_{\text{cr}}^{\text{b}} = -E_{\text{cr}}^{\text{disl}}$  is the binding energy of dislocation with the crowdion ( a precise equation can be found in [34]). So,  $t_{\text{leave}} < t_{\text{ab}}$  estimated above if  $E_{\text{cr}}^{\text{b}} < E_{\text{db}}^{\text{f}} - E_{\text{cr}}^{\text{f}} + E_{\text{db}}^{\text{m}} = 0.3 \text{ eV}$ .

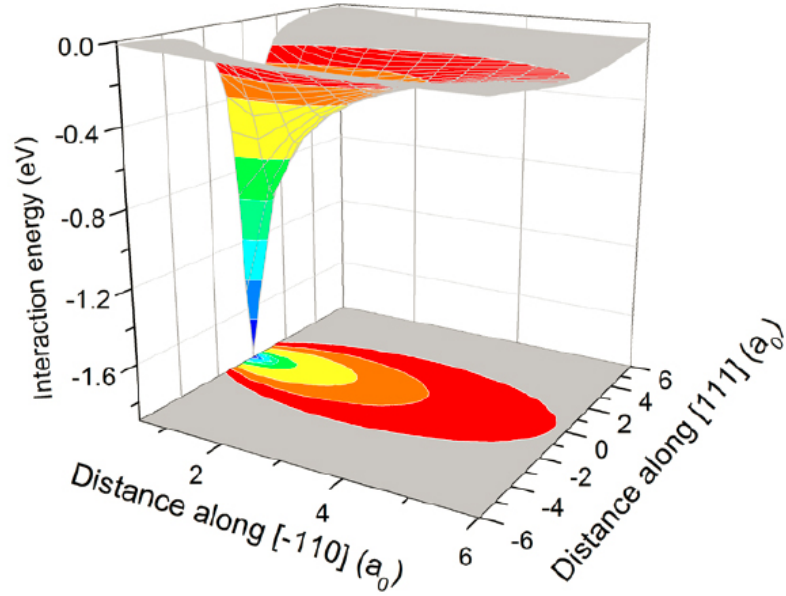


Figure 5. The energy landscape for a vacancy near the  $\frac{1}{2}[111](\bar{1}10)$  edge dislocation in Mo.

As a final note to this Section, let us show that supposition made in [21] that a low density of jogs on the dislocation line can affect significantly the sink strength of dislocations is wrong. Assume a vacancy (or an SIA) is already near the dislocation line but it has to move a distance  $n^{-1}$  towards nearest jog. It would take approximately  $(n)^{-2} / 6D_v$  to reach this point. The time required to dissociate from dislocation line to the matrix is  $\left( \frac{L_v}{a_0} \right)^2 \exp(-\beta E_v^{\text{f}}) / 6D_v$ . So, for  $L_v \approx 10 a_0$  and  $E_v^{\text{f}} = 2 \text{ eV}$ , these times are equal to each other if the distance between jogs is of the order of  $n^{-1} \approx 6 \times 10^5 a_0 = 50 \mu\text{m}$  for  $T = 820^\circ\text{C}$ , and even longer for lower temperature, which is unrealistic. The results obtained in [21], in particular Figure 2 on page 1400 which suggests high sensitivity of swelling rate to the jog density in the region of  $n^{-1} \approx 50 a_0$ , must be erroneous.

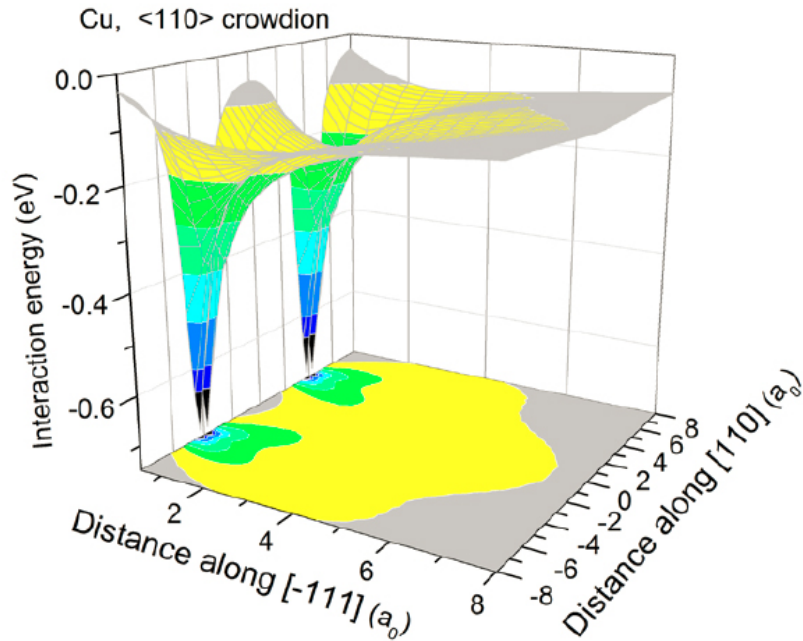


Figure 6. The interaction energy landscape of a  $\frac{1}{2}[110]$  crowdion in the expansion region below the line of a perfect  $\frac{1}{2}[110](\bar{1}11)$  edge dislocation in copper.

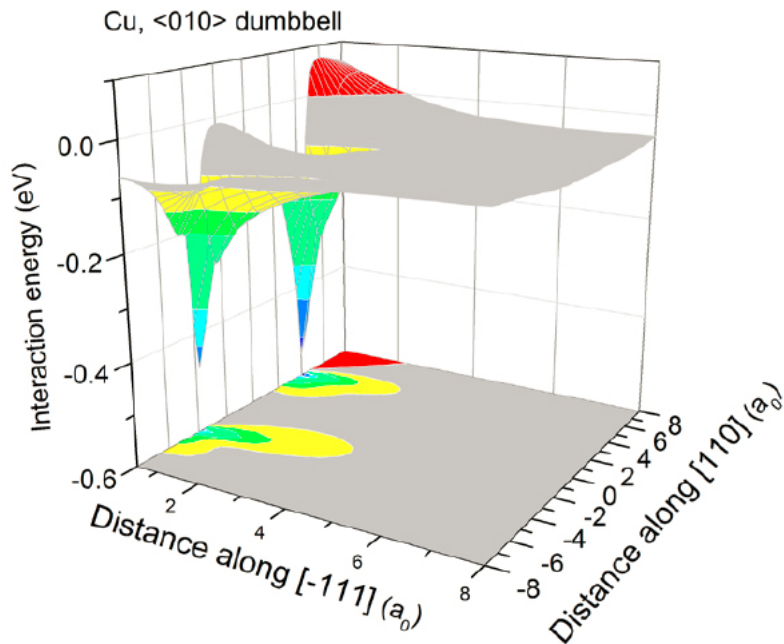


Figure 7. The interaction energy landscape of a  $[010]$  dumbbell in the expansion region below the line of a perfect  $\frac{1}{2}[110](\bar{1}11)$  edge dislocation in copper.

### C. Copper

For Cu, the situation is similar with two exceptions. First, the  $\frac{1}{2}\langle 110 \rangle (111)$  edge dislocation is extended due to relatively small stacking-fault energy,  $\sim 40 \text{ mJ/m}^2$ : the two partials being separated by about  $11b$  (see [35], pp.87-89). Second, the  $\langle 100 \rangle$ -dumbbell configuration in pure crystal is more stable than the  $\frac{1}{2}\langle 110 \rangle$  crowdion configuration. The difference should not be very large and the SIA will frequently assume the crowdion configuration and migrate along its axis. Hence, in the vicinity

of dislocation core there should be difficult for the SIA to jump towards the dislocation line and the SIA may leave the dislocation region in crowdion configuration.

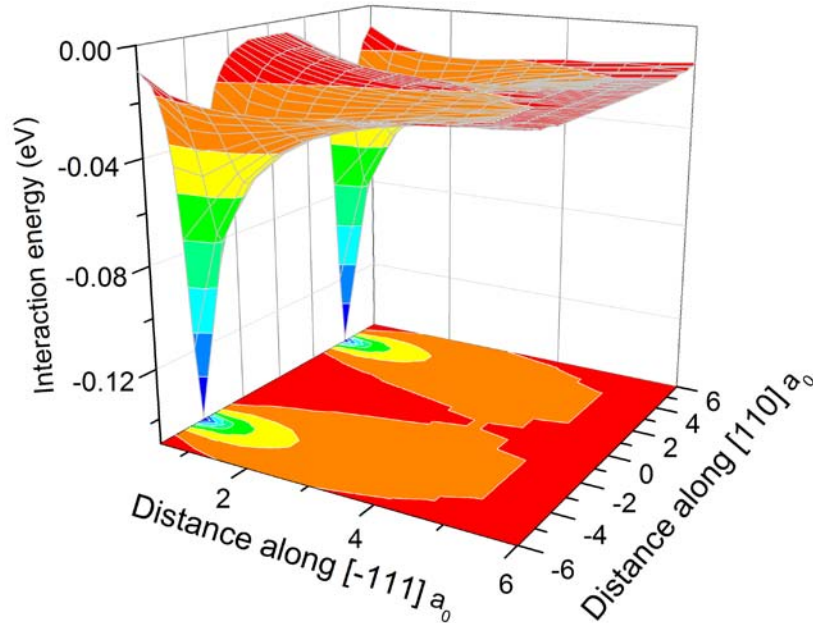


Figure 8. The interaction energy landscape of a vacancy in the compression region above the line of a perfect  $\frac{1}{2}[110](\bar{1}11)$  edge dislocation in copper.

Figure 6 shows the interaction energy landscape for the crowdion configuration with the axis parallel to the dislocation Burgers vector. As can be seen, the interaction energy is much smaller in Cu than in Mo. This fact (generally for the fcc compared to bcc lattices) has already been noticed by Kuramoto in [24] and is because of the extended dislocation and smaller shear modulus (see Table 1). Thus, although the values  $\mu\Delta\Omega_i$  are similar in Cu and Mo and the interaction energy is predicted by Eq. (4) to be similar, it is, in fact, weaker in Cu due to dissociation of dislocation. This is valid for the vacancies as well (see Fig. 8). In addition, similar to Mo, the interaction energy of dislocation with the most stable dumbbell configuration (see Fig. 7) is smaller than that for the crowdion. This shows a qualitative difference in the mechanisms controlling the dislocation bias from those in the conventional theory. Note that despite the stronger interaction of the SIAs with dislocations in Mo, the bias factor in Mo may be smaller than that in Cu due to higher stability of crowdions compared to dumbbells and the 1-D mobility of crowdions along the dislocation Burgers vector.

#### IV. Generalised diffusion equations

A way of writing equations for the concentrations of SIAs for a simplified scenario, which account, however, for the existence of different SIA configurations is as follows. Let us assume that dumbbells migrate along the  $x$  coordinate towards the dislocation located at  $x=0$ , while crowdions migrate along transverse  $y$  coordinate parallel to the dislocation Burgers vector (see Fig. 6). Then, in the framework described in Section 2 (absence of the generation term and with the boundary conditions described by Eqs. (5) and (6)), the concentrations of dumbbells,  $C_{db}$ , and crowdion configurations,  $C_{cr}$ , are described by the usual continuity equations containing additional term describing mutual transformations

$$\frac{dC_{db}}{d\phi} = -(\nu_{db \rightarrow cr} C_{db} - \nu_{cr \rightarrow db} C_{cr}) - \nabla J_{db}, \quad (14)$$

$$\frac{dC_{cr}}{d\phi} = (\nu_{db \rightarrow cr} C_{db} - \nu_{cr \rightarrow db} C_{cr}) - \nabla J_{cr}, \quad (15)$$

where  $J_{db}$  and  $J_{cr}$  are the corresponding fluxes of SIAs, and  $\nu_{db \rightarrow cr} \propto \exp[-\beta(E_{db}^f - E_{cr}^f)]$  is the rate by which a dumbbell is transformed into crowdion, and  $\nu_{cr \rightarrow db} \propto \exp[-\beta(E_{cr}^f - E_{db}^f)]$  is the rate of the reverse reaction.

Let us consider limiting cases. If the dumbbell configuration is much more stable than the crowdion configuration, then  $C_{cr} = 0$  and  $\nu_{db \rightarrow cr} = 0$ , hence the first terms in the right-hand side of Eq. (14) and Eq. (15) itself are zero. The remaining terms represent usual continuity equation in the system of migrating dumbbell SIAs, as in the case considered by Heald [6] (see Section 2).

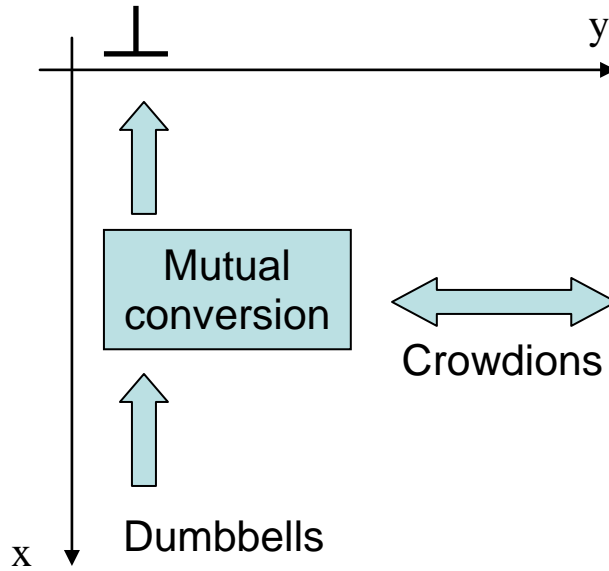


Figure 9. Diagram illustrating a simplified scenario of SIA diffusion near dislocation, which includes mutual conversions of SIA dumbbell and crowdion configurations.

In the case, when the dumbbell configuration is still more stable than the crowdion configuration in the matrix but with crowdion configuration stabilized near the dislocation line, the dumbbells may be converted into the crowdion configuration and leave the region, i.e. escape to the matrix, without being absorbed by the dislocation. In this situation, not all dumbbells entering the region, where the interaction energy with the dumbbell is greater than the thermal energy, join the dislocation line: some would escape in crowdion configuration. The effective capture radius of dislocation for the SIAs is smaller in this case than that defined by the equality of the interaction energy to the thermal energy. And the dislocation bias factor is smaller than that defined by Eq. (8).

If the crowdion configuration is much more stable than the dumbbell configuration, then the SIA diffusion is pure 1-D. This situation is described by the PBM [13-15], where the dislocation capture distance for an SIA,  $r_D$ , defines zone of spontaneous absorption, and is, hence, much smaller than  $L_1$  (see [36], page 99). In addition, after some irradiation dose, a saturation of swelling may be achieved for the void radius  $r_{void} \approx 2\pi r_D$  for a random void arrangement. In this case, the

transformation of crowdion to dumbbell configuration may increase the dislocation capture radius for the SIAs. This is in contrast to the situation when the dumbbells are more stable, and their transformation to crowdion configuration leads to a decrease of the effective capture radius. In both the cases, however, the capture radius is smaller than  $L_i$  while the dislocation bias smaller than that given by Eq. (8).

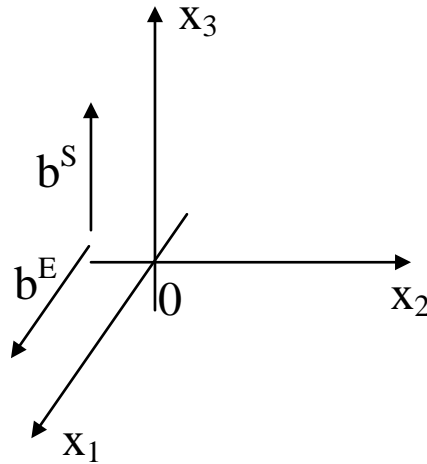


Figure 10. Coordinate system for calculating stress field around a dislocation with the edge,  $\mathbf{b}^E$ , and screw,  $\mathbf{b}^S$ , components of the Burgers vector.

## SUMMARY of RESULTS

The main results can be summarized as follows:

1. Large dislocation bias factors as compared to those derived from the swelling rates observed in the framework of the conventional theory are a consequence of the assumption that the SIAs migrate 3-D in the vicinity of dislocation line and correspond to maximum values in the cases when the assumption is correct.
2. An assumption of the low density of jogs on dislocation line cannot resolve the contradiction.
3. The 1-D migration of the crowdions with axes parallel to the dislocation Burgers is a process controlling the SIA absorption by the dislocation, hence, the damage accumulation driven by the dislocation bias. The key aspect is an increased probability for the SIAs to escape from the capture region to the matrix, hence decreasing the effective capture radius.
4. The dislocation capture radius for SIAs is determined by the relative stability of the crowdion and dumbbell configurations. The corresponding energy criterion is stronger than the equality of interaction energy to the thermal energy, as in the case of pure 3-D diffusion. This leads to reduced bias factors as required by experiments.
5. Dissociation of dislocations in the fcc metals may be an additional reason for the reduced values of the dislocation bias.
6. The analysis suggests categorizing metals according to relative stability of the SIA crowdion configuration and sheds light on possible reasons for the higher swelling levels observed in fcc compared to bcc materials.
7. Different metals have wide range of relative stability of the crowdion and dumbbell SIA configurations. The diffusion-reaction kinetics in these metals may, thus, vary from that corresponding to pure 1-D migration to that of 3-D diffusion of irradiation-produced defects. The former should be similar to that under neutron irradiation, where the displacement cascades produce 1-D migrating SIA clusters, and described by the PBM (see, e.g. [13,15]).

It is worthy to emphasize that the analysis presented illuminates similarity of the damage mechanisms operating under electron and neutron / heavy ion irradiations: in both cases the 1-D migration of interstitial defects plays key role in the microstructure evolution. In this context, the decoration of dislocations with the cascade-produced SIA clusters may be viewed as a magnified analogy to the behaviour of single SIAs near dislocation. While here we have shown that the presence of 1-D diffusion reduces the dislocation bias factor, in [37] we argue that the decoration may even account for the damage saturation observed in metals. Here we presented a very general analysis of the problem. A combination of first principle, MD and kMC calculations is required to investigate details of point-defect interaction with dislocations and calculate dislocation bias factors in different materials under different conditions.

Finally, let us note that, the very use of metallic alloys as structural materials for nuclear applications becomes possible due to existence of crowdions. Otherwise, high swelling rates would eliminate this possibility. In the latter case, the bias factors would be so large that, despite intra-cascade recombination and clustering, it would be dominant driving force for the damage accumulation even under neutron irradiation (see [15], section 2), and lead unacceptable swelling rates.

## ACKNOWLEDGEMENTS

The research was sponsored by the Office of Fusion Energy Sciences U.S. Department of Energy, under contract DE-AC05-00OR22725 with UT-Battelle, LLC (S.I.G.).

## REFERENCES

- [1] G.W. Greenwood, A.J.E. Foreman, D.E. Rimmer, *J. Nucl. Mater.* 4 (1959) 305.
- [2] C.C. Cawthorne, E.J. Fulton, *Nature* 216 (1967) 575.
- [3] A.D. Brailsford, R. Bullough, *Philos. Trans. R. Soc. London A* 302 (1981) 87.
- [4] R. Bullough, B.L. Eyre, R.C. Perrin, *Nucl. Appl. and Technology* 9 (1970) 346.
- [5] A.J.E. Foreman, Harwell report AERE-R-7629 (1974).
- [6] P.T. Heald, *Philos. Mag.* 31 (1975) 551.
- [7] F.S. Ham, *J. Appl. Phys.* 30 (1959) 915.
- [8] I.G. Margvalashvili, Z.K. Saralidze, *Sov. Phys. Solid State* 15 (1974) 1774.
- [9] P.T. Heald, K.M. Miller, *J. Nucl. Mater.* 66 (1976) 107.
- [10] R.J. White, S.B. Fisher, P.T. Heald, *Philos. Mag.* 34 (1976) 647.
- [11] K.M. Miller, *J. Nucl. Mater.* 84 (1979) 167.
- [12] W.G. Wolfer, *J. Computer-Aided Mater. Des.* 14 (2007) 403.
- [13] S.I. Golubov, B.N. Singh, H. Trinkaus, *Philos. Mag. A* 81 (2001) 2533.
- [14] B.N. Singh, M. Eldrup, A. Horsewell, P. Ehrhart, F. Dworschak, *Philos. Mag. A* 80 (2000) 2629.
- [15] A.V. Barashev, S.I. Golubov, *Philos. Mag.* 89 (2009) 2833.
- [16] P. Barlow, DPhil Thesis, University of Sussex (1977).
- [17] Yu.V. Konobeev, S.I. Golubov, In: R.E. Stoller, A.S. Kumar, D.S. Gelles (eds.) *Proc. of the 15th Int. Symp. on Effects of Radiation on Materials*, ASTM STP 1125 (1992) (Philadelphia, Pennsylvania: ASTM), p. 569.
- [18] L.D. Glowinski, *J. Nucl. Mater.* 61 (1976) 8.
- [19] G.P. Walters, *J. Nucl. Mater.* 136 (1985) 263.
- [20] N. Igata, A. Kohyama, S. Nomura, *J. Nucl. Mater.* 103-104 (1981) 1157.
- [21] R. Bullough, T.M. Quigley, *J. Nucl. Mater.* 10-104 (1981) 1397.
- [22] G.J. Ackland, D.J. Bacon, A.F. Calder, T. Harry, *Philos. Mag. A* 75 (1997) 713.
- [23] K. Makii, T. Tsutsumi, Y. Aono, E. Kuramoto, *Mater. Trans. JIM* 30 (1989) 505.

- [24] E. Kuramoto, J. Nucl. Mater. 191-94 (1992) 1279.  
 [25] H. Kamiyama, H Rafii-Tabar, Y Kawazoe, H Matsui, J. Nucl. Mater. 212-215 (1994) 231.  
 [26] E. Kuramoto, K. Ohsawa, T. Tsutsumi, J. Nucl. Mater. 283-287 (2000) 778.  
 [27] A.H. Cottrell, Report on Strength of Solids, Physical Society, London 30 (1948).  
 [28] B.A. Bilby, Proc. Phys. Soc. A 63 (1950) 3.  
 [29] D. Nguyen-Manh, A.P. Horsfield, S.L. Dudarev, Phys. Rev. B 73 (2006) 020101(R).  
 [30] C. Domain and C.S. Becquart, Phys. Rev. B 65 (2002) 024103.  
 [31] C.C. Fu, F. Willaime, P. Ordejon, Phys. Rev. Lett. 92 (2004) 175503.  
 [32] M.J. Makin, Philos. Mag. 10 (1964) 695.  
 [33] J.P. Hirth, J. Lothe, Theory of dislocations, McGraw-Hill Book Company (1968) p.762.  
 [34] A.V. Barashev, S.I. Golubov, Yu.N. Osetsky, R.E. Stoller, Philos. Mag. 90 (2010) 907.  
 [35] D. Hull, D.J. Bacon, Introduction to dislocations (Butterworth-Heinemann, Oxford, 2001), 4th ed.  
 [36] H. Trinkaus, B.N. Singh, A.J.E. Foreman, J. Nucl. Mater. 249 (1997) 91.  
 [37] S.I. Golubov, A.V. Barashev, B.N. Singh, in preparation.

### APPENDIX A. Long-range forces between dislocation loop and edge dislocation

When a straight dislocation lies along  $x_3$  direction with the screw component of the Burgers vector,  $\mathbf{b}^S$ , along  $x_3$  and the edge component,  $\mathbf{b}^E$ , along  $x_1$  (see Fig. 1), then the components of the stress tensor are given by the relations [32]:

$$\sigma_{11} = \frac{-Dx_2(3x_1^2 + x_2^2)}{(x_1^2 + x_2^2)^2}, \quad \sigma_{12} = \frac{Dx_1(x_1^2 - x_2^2)}{(x_1^2 + x_2^2)^2} \quad (\text{A1})$$

$$\sigma_{22} = \frac{Dx_2(x_1^2 - x_2^2)}{(x_1^2 + x_2^2)^2}, \quad \sigma_{13} = \frac{-Sx_2}{x_1^2 + x_2^2}, \quad (\text{A2})$$

$$\sigma_{33} = \frac{-2\nu Dx_2}{x_1^2 + x_2^2}, \quad \sigma_{23} = \frac{Sx_1}{x_1^2 + x_2^2}, \quad (\text{A3})$$

where

$$D = \mu \mathbf{b}^E / 2\pi(1 - \nu) \text{ and } S = \mu \mathbf{b}^S / 2\pi, \quad (\text{A4})$$

where  $\mu$  is the shear modulus and  $\nu$  is Poisson's ratio. The remaining components obey the rule,  $\sigma_{ij} = \sigma_{ji}$ , where  $\sigma_{ij}$  is the stress in the  $i$  direction on an area perpendicular to the  $j$  axis.

If stress components are constant over the area of a small loop, the interaction energy is the sum of each of the stress components multiplied by both the loop area resolved in the appropriate direction and the displacement produced by the loop:

$$E = A' \sum \sigma_{ij} b'_i n'_j, \quad (\text{A5})$$

where  $b'_i$  is the component of the loop Burgers vector in the  $i$  direction and  $A'n'_j$  is the area of the loop resolved onto a plane perpendicular to the  $j$  direction.

MIT OpenCourseWare  
<http://ocw.mit.edu>

22.14 Materials in Nuclear Engineering  
Spring 2015

For information about citing these materials or our Terms of Use, visit: <http://ocw.mit.edu/terms>.